

## **Title page**

# **Discovery and Validation of Nitroxoline as a Novel STAT3 Inhibitor in Drug-resistant Urothelial Bladder Cancer**

Wenfeng Lin<sup>1</sup>, Jingkai Sun<sup>1,2</sup>, Takuya Sadahira<sup>1</sup>, Naijin Xu<sup>1,3</sup>, Koichiro Wada<sup>1</sup>,  
Chunxiao Liu<sup>2</sup>, Motoo Araki<sup>1</sup>, Abai Xu<sup>2</sup>, Masami Watanabe<sup>1,4</sup>, Yasutomo Nasu<sup>1</sup>, Peng  
Huang<sup>1,2,5</sup>

<sup>1</sup>Department of Urology, Okayama University Graduate School of Medicine,  
Dentistry and Pharmaceutical Sciences, Okayama, Japan;

<sup>2</sup>Department of Urology, Zhujiang Hospital, Southern Medical University, Guangzhou,  
China;

<sup>3</sup>Department of Urology, Sir Run Run Shaw Hospital, Zhejiang University School of  
Medicine, Hangzhou, China;

<sup>4</sup>Center for Innovative Clinical Medicine, Okayama University Hospital, Okayama,  
Japan;

<sup>5</sup>Okayama Medical Innovation Center, Okayama University, Okayama, Japan.

## **Corresponding author:**

Peng Huang M.D Ph.D

Department of Urology, Okayama University Graduate School of Medicine, Dentistry  
and Pharmaceutical Sciences, Okayama 700-8558, Japan

Tel + 81-86-235-7997; Fax +81-86-235-7884

Email : [huangpeng509@gmail.com](mailto:huangpeng509@gmail.com)

## **Abstract**

Repeated cycles of first-line chemotherapy drugs such as doxorubicin (DOX) and cisplatin (CIS) trigger frequent chemoresistance in recurrent urothelial bladder cancer (UBC). Nitroxoline (NTX), an antibiotic to treat urinary tract infections, has been recently repurposed for cancer treatment. Here we aimed to investigate whether NTX suppresses drug-resistant UBC in vitro and in vivo and its molecular mechanism. The drug-resistant cell lines T24/DOX and T24/CIS were established by continual exposure of parental cell line T24 to DOX and CIS, respectively. T24/DOX and T24/CIS cells were resistant to DOX and CIS, respectively, but they were sensitive to NTX time- and dose-dependently. Overexpressions of STAT3 and P-glycoprotein (P-gp) were identified in T24/DOX and T24/CIS, which could be reversed by NTX. Furthermore, western blot showed that NTX downregulated the expressions of phosphorylated STAT3, c-Myc, Cyclin D1, CDK4, CDK6, Bcl-xL, Mcl-1, and Survivin, which were further confirmed by Stattic. In vivo, NTX exhibits the significant anti-tumor effect in T24/DOX and T24/CIS tumor-bearing mice. These results suggested that NTX-induced G0/G1 arrest, apoptosis, and P-gp reversal in drug-resistant UBC were mediated by inhibition of STAT3 signaling. Our findings repurpose NTX as a novel STAT3 inhibitor to induce P-gp reversal, G0/G1 arrest, and apoptosis in drug-resistant UBC.

**Keywords:** Urothelial bladder cancer, doxorubicin, cisplatin, chemoresistance, nitroxoline, STAT3.

## **Introduction**

Urothelial bladder cancer (UBC) is a malignant tumor originating primarily from the transitional cells of bladder urothelium [1]. According to the Cancer Statistics, 2021, it has been estimated that there would be 83,730 new cases of UBC, and that 17,200 patients would die of this disease in the United States [2]. Although muscle-invasive bladder cancer (MIBC) accounts for 20-30% of the newly diagnosed UBC cases, it is responsible for the vast majority of UBC-specific deaths [3]. Moreover, 50%-70% of non-muscle-invasive bladder cancer (NMIBC) cases will recur after transurethral resection, while 10-30% will progress to MIBC [4]. Therefore, UBC is characterized by the high rate of recurrence, progression, and mortality, leading to poor treatment results and heavy economic burden. Adjuvant chemotherapy has been extensively applied for patients with UBC, which helps to improve their overall survival and quality of life [5]. Both doxorubicin (DOX/ADM/ADR) and cisplatin (CIS/DDP/CDDP) have been the first-line chemotherapy drugs effectively against UBC, but the high rates of DOX- and CIS- chemoresistance in recurrent UBC remain a major barrier to improve the prognosis of patients [6, 7]. Atezolizumab, an antibody against programmed cell death ligand-1 (PD-L1), and pembrolizumab, an antibody against programmed cell death protein 1 (PD-1), have obtained accelerated approval in cisplatin-ineligible population with advanced urothelial carcinoma. Although atezolizumab and pembrolizumab have a confirmed objective response rate of 23.5% in IMvigor210 trial and 28.6% in KEYNOTE-052 trial, respectively [8], it still

maintains a challenge to explore novel effective chemotherapeutic agents for the treatment of drug-resistant UBC.

Multidrug resistance (MDR), a clinical obstacle to the long-term success of chemotherapy, represents the cross-resistance of tumor cells to various chemotherapeutic agents with different structures and functions [9]. One of the main reasons for MDR phenotype is the overexpression of P-glycoprotein (P-gp), which is a 170 kDa transmembrane glycoprotein encoded by the ATP-binding cassette B1 (ABCB1) gene, also known as multidrug resistance 1 (MDR1) gene [10]. As a drug efflux pump, P-gp extrudes its substrates such as DOX out of tumor cells, thus resulting in a reduction of intracellular drug concentration [11]. P-gp has also been reported to reduce the tumor sensitivity to the non-P-gp substrates such as CIS, while inhibition of P-gp has the potential to increase CIS sensitivity [12, 13]. Signal transducer and activators of transcription 3 (STAT3) acts as a crucial transcription factor to regulate its downstream target genes, which subsequently involves in diverse biological processes such as cell proliferation, survival, and chemoresistance [14]. Overexpression and activation of STAT3 correlate with the poor prognosis of UBC [15, 16], and STAT3 requires the phosphorylation at the residues of Tyr705 (p-STAT3 (Y705)) and Ser727 (p-STAT3 (S727)) for its maximal activation [17]. The chromatin immunoprecipitation (ChIP) assay demonstrated that STAT3 can bind to the potential promoter region of MDR1, and increasing evidence suggests that inhibiting STAT3 activation effectively downregulates the expression of P-gp [18, 19]. Based on the above research evidence, the development of potent inhibitors targeting STAT3

signaling may be a promising therapeutic strategy against drug-resistant UBC. Although multiple inhibitors targeting STAT3 in cancer have been identified in preclinical and early phase clinical trials, the potential low efficacy or adverse effects may limit their clinical transformation [20].

Drug repurposing, also known as drug repositioning, refers to discovering novel indications of the currently marketed drugs which have been applied to treat other diseases [21]. Nitroxoline (NTX), an antibiotic used clinically to treat urinary tract infections, has been repurposed for the treatment of multiple tumors such as UBC [22-24], pancreatic cancer [25], and glioma [26]. Several studies have reported its anti-tumor activity against UBC since Shim and coworkers firstly identified NTX as an antiangiogenic agent in UBC through inhibition of methionine aminopeptidase-2 (MetAP2) [22-24]. In an orthotopic mouse model, NTX was demonstrated to exhibit anti-UBC effect with favorable safety profile and pharmacokinetic properties [24]. Our previous study has also revealed that NTX suppresses the progression of UBC by reversing epithelial-mesenchymal transition (EMT) and enhancing anti-tumor immunity [23]. Prior studies have noted that P-gp expression is identified in pre-chemotherapy UBC tissue samples, which increases with MDR after chemotherapy [27, 28]. However, it has not been reported whether NTX and its analogues suppress the growth of drug-resistant UBC. And the mechanism whether NTX inhibits STAT3 signaling and reverses P-gp overexpression remains to be explored at the molecular level.

Drug repurposing of NTX in drug-resistant UBC may contribute to the following

advantages including its well-known drug properties (pharmacokinetics, efficacy, toxicity and drug interactions), developing a putative agent with fewer funds and shorter period [24]. Therefore, this study was designed to explore the potential anti-tumor characteristics of NTX in drug-resistant UBC and the possible molecular mechanism. The cell lines of drug-resistant UBC were established by continually exposing the parental cell line T24 (derived from MIBC) to DOX (T24/DOX) and CIS (T24/CIS). Both in vitro and in vivo experiments were then performed to investigate whether NTX could reverse P-gp overexpression and effectively inhibit the growth of T24/DOX and T24/CIS cells through regulation of STAT3 signaling. Our findings could have significant clinical implications in repurposing NTX as a STAT3 signaling inhibitor against drug-resistant UBC.

## **Material and Methods**

### **Chemicals and antibodies**

The chemicals including DOX and CIS were purchased from MedChemExpress (MCE, New Jersey, USA). Both DOX and CIS were dissolved in phosphate buffered saline (PBS), followed by ultrasonic bath and filtration through a 0.22- $\mu$ m filter (Millipore, USA). Nitroxoline was provided by Jiangsu Asieris Pharmaceuticals, Co., Ltd. (Taizhou, Jiangsu, China). It was dissolved in phosphate buffered saline (PBS) and then filtered through a 0.22- $\mu$ m filter. Stattic, a selective inhibitor of STAT3 activation and dimerization, was obtained from Tocris Bioscience (#2978, Bristol, UK), which was dissolved in dimethyl sulfoxide (DMSO) with a stock solution of 20

mM stored at -20°C. The primary antibodies against STAT3 (#12640), p-STAT3 (Y705) (#9145), p-STAT3 (S727) (#9134), MDR1/P-gp (#13342), c-Myc (#5605), Cyclin D1 (#2978), CDK4 (#2906), CDK6 (#3136), Bcl-xL (#2764), Mcl-1 (#4572), Survivin (#2808), and  $\beta$ -Actin (#4970) were purchased from Cell Signaling Technology (CST, Beverly, MA, USA). The secondary antibodies were anti-rabbit IgG, HRP-linked antibody (#7074) and anti-mouse IgG, HRP-linked antibody (#7076) from CST.

### **Drug-resistant cell lines and cell culture**

Human bladder cancer cell line T24 was purchased from the American Type Culture Collection (ATCC, Manassas, VA, USA). DOX-resistant bladder cancer cell line T24/DOX and CIS-resistant bladder cancer cell line T24/CIS were established from our laboratory based on continual exposure of parental cell line T24 to the culture media with DOX and CIS, respectively [29-31]. T24, T24/DOX, and T24/CIS cells were cultured in Dulbecco's modified eagle medium (DMEM, Invitrogen, USA) supplemented with 10% fetal bovine serum (FBS, Invitrogen, USA), 1% penicillin-streptomycin (Invitrogen, USA) and were incubated at 37°C in a humidified atmosphere with 5% CO<sub>2</sub>. To maintain the drug-resistant characteristics, T24/DOX cells were cultured with 1  $\mu$ M DOX while T24/CIS cells were cultured with 10  $\mu$ M CIS prior to experiment.

### **Cell viability assay**

T24, T24/DOX, and T24/CIS cells were seeded in 96-well plates at  $2 \times 10^3$  per well and allowed to attach overnight. For drug sensitivity analysis, T24 and T24/DOX cells

were treated with different concentrations of DOX (0, 0.1, 1, 10, 20, and 100  $\mu\text{M}$ ) for 24 h, while T24 and T24/CIS cells were treated with different concentrations of CIS (0, 10, 20, 40, and 80  $\mu\text{M}$ ) for 24 h. To determine the effect of NTX on cell proliferation, T24, T24/DOX, and T24/CIS cells were exposed to NTX at the concentrations of 0, 2.5, 5, 10, 20, and 40  $\mu\text{M}$  for 24, 48, and 72 h. At the indicated treatment time points, the culture media were removed and the cells were washed gently once with PBS. The prepared XTT working solution (Cell Proliferation Kit II, #11465015001, Sigma-Aldrich) was added to the cells, which were subsequently incubated at 37 °C for 4-24 h. Finally, the optical density (OD) levels were determined by the Model 680 Microplate Reader (Bio-Rad, Hercules, USA).

### **Hoechst 33342 staining**

Hoechst staining was applied to identify such morphological changes as nuclear fragmentation and chromatin condensation. T24, T24/DOX, and T24/CIS cells ( $2 \times 10^5$  per well) were seeded in 6-well plates and cultured for 24 h. After 48 h treatment with 0 and 40  $\mu\text{M}$  NTX, the cells were stained at room temperature for 20 min with Hoechst 33342 (#H3570, ThermoFisher Scientific, USA) at a final concentration of 5  $\mu\text{g/ml}$ . Next, the occurrence of apoptotic cells was observed directly under fluorescence microscope.

### **Cell cycle distribution analysis**

T24, T24/DOX, and T24/CIS cells were seeded in 6-well plates at a density of  $2 \times 10^5$  cells per well. After incubated with NTX (0, 10, 20, or 40  $\mu\text{M}$ ) for 24 h, the cells were then harvested, washed twice with PBS and fixed in precooling 70% ethanol at 4°C



for over 18 h. Subsequently, they were rinsed twice with the first time in PBS and the second one in stain buffer (#554656, BD Biosciences). The cells were further incubated in PI/RNase staining buffer (#550825, BD Biosciences) at room temperature for 15 min, followed by the detection using MACSQuant Analyzer 10 (Miltenyi Biotec, Cologne, Germany) and the analysis using MACSQuantify™ Software 2.6.

### **Annexin V-FITC/PI staining for apoptosis detection**

T24, T24/DOX, and T24/CIS cells were seeded in 6-well plates at  $1.5 \times 10^5$  cells per well. After 48 h treatment with NTX (0, 10, 20, or 40  $\mu\text{M}$ ), cells were collected, rinsed twice with PBS and then resuspended in 1X Annexin V binding buffer to obtain a density of  $1 \times 10^6$  cells/ml. Then 100  $\mu\text{l}$  of the cell suspension was incubated with 5  $\mu\text{l}$  of FITC Annexin V and 5  $\mu\text{l}$  of PI (#556547, BD Biosciences) in the dark at room temperature for 15 min. Finally, cell apoptosis was examined by MACSQuant Analyzer 10 and analyzed by MACSQuantify™ Software 2.6.

### **Western blot analysis**

The total proteins were extracted using M-PER™ Mammalian Protein Extraction Reagent (#78501, ThermoFisher Scientific, USA) and then quantified by Bradford protein assay. The same amount of protein (10  $\mu\text{g}/\text{well}$ ) was separated by 10% or 12% Mini-PROTEAN TGX Precast Protein Gels and then transferred to 0.2  $\mu\text{m}$  PVDF Transfer Packs (#1704156, Bio-Rad, USA) on the Trans-Blot Turbo transfer system (#170-4155, Bio-Rad, USA). The membranes were blocked with 5% non-fat milk or bovine serum albumin for 1.5 h at room temperature and then incubated with the

primary antibodies described above at 4°C overnight. After rinsing with 1X TBST, the membranes were incubated with the indicated secondary antibody for 1.5 h at room temperature. Protein visualization was performed using ECL detection reagent (#RPN2232, GE Healthcare) and ChemiDoc Imaging System (Bio-Rad, USA).  $\beta$ -actin was used as an internal control.

### **Subcutaneous xenograft models of T24/DOX and T24/CIS**

Male BALB/c nude mice (five-week-old) were provided by Japan SLC, Inc. (Shizuoka, Japan) and maintained in specific pathogen-free (SPF) conditions. The mice experimentation was performed in compliance with the Animal Care and Use Committee, Okayama University.

T24/DOX cells ( $1 \times 10^6$ ) or T24/CIS cells ( $1 \times 10^6$ ) were resuspended in 100  $\mu$ l mixture (1:1) of Hank's buffered saline solution (HBSS) and Matrigel (BD Biosciences, USA), followed by the subcutaneous inoculation into the right flank of mice. When tumor volume reached approximately 100 mm<sup>3</sup>, T24/DOX tumor-bearing mice were randomized into two groups (n = 6 for each group) and assigned to orally receive vehicle (PBS) or NTX (40 mg/kg) once every day for two weeks prior to sacrifice. It was the same with T24/CIS tumor-bearing mice. Both mouse body weight and tumor growth were measured twice a week. Tumor volume was calculated using this formula: Volume = width<sup>2</sup>  $\times$  length  $\times$  0.52. At the endpoint, the tumors were surgically removed, weighed, and photographed. Protein from tumor tissue was extracted using T-PER Tissue Protein Extraction Reagent (#78510, ThermoFisher Scientific, USA), which was subsequently analyzed by western blot analysis

mentioned above. For histological examination, tumor tissues were fixed with 10% formaldehyde, embedded in paraffin and cut into 4  $\mu\text{m}$  sections. The sections were stained with hematoxylin and eosin (H&E) staining to observe the morphological alterations after NTX treatment.

### **Statistical analysis**

Each experiment was repeated at least three times and data are expressed as mean  $\pm$  standard deviation (SD). GraphPad Prism 8.3 software was used to perform all statistical analyses including the calculation of half maximal inhibitory concentration (IC<sub>50</sub>) and the creation of statistical charts. Between-group difference was assessed by Student's t-test or one-way analysis of variance (ANOVA). A *P* value < 0.05 was considered to be statistically significant.

## **Results**

### **Characterization of DOX-resistant and CIS-resistant bladder cancer cell lines**

To confirm whether bladder cancer cell lines acquired resistance to DOX or CIS, the viability of T24/DOX or T24/CIS cells was determined by XTT assay following the indicated treatment for 24 h. Although DOX dose-dependently inhibited the proliferation of T24/DOX cells, the sensitivity to DOX was lower than that of parental T24 cells (**Figure 1A**). For DOX, the IC<sub>50</sub> value in T24 cells was 0.71  $\mu\text{M}$  [95% confidence interval (95%CI), 0.56-0.89], while that in T24/DOX cells was 10.93  $\mu\text{M}$  (95%CI, 6.88-17.55), with a 15.4-fold change in IC<sub>50</sub> (**Table 1**). Similarly, CIS dose-dependently inhibited the proliferation of T24/CIS cells, but the sensitivity to

CIS was lower than that of parental T24 cells (**Figure 1B**). For CIS, the IC<sub>50</sub> value in T24 cells was 16.27  $\mu$ M (95%CI, 13.29-19.11), while that in T24/CIS cells was 58.04  $\mu$ M (95%CI, 51.11-67.55), with a 3.6-fold change in IC<sub>50</sub> (**Table 1**).

We next analyzed the expressions of STAT3 and P-gp by western blot. As shown in **Figure 1C**, the levels of STAT3 and P-gp were upregulated in T24/DOX and T24/CIS cells compared with T24 parental cells.

### **NTX inhibits the proliferation of DOX-resistant and CIS-resistant bladder cancer cells**

The dose- and time-dependent inhibitions were observed in the viability of T24 parental cells (**Figure 1D**), and drug-resistant cell lines T24/DOX (**Figure 1E**), T24/CIS (**Figure 1F**). Moreover, for 48 h treatment of NTX, the IC<sub>50</sub> values in T24/DOX (10.69  $\mu$ M) and T24/CIS (11.20  $\mu$ M) were slightly higher than that in T24 cells (7.85  $\mu$ M), but there was no significant difference in IC<sub>50</sub> values of NTX between T24 parental cells and drug-resistant cells (**Table 1**).

### **NTX triggers G0/G1 phase arrest in DOX-resistant and CIS-resistant bladder cancer cells**

To examine whether NTX inhibited the cell cycle progression, T24, T24/DOX, and T24/CIS cells were treated with different concentrations of NTX for 24 h, followed by flow cytometric analysis (**Figure 2A**). As drug concentration increased, a higher percentage of cells stayed at G0/G1 phase, while a lower percentage of cells stayed at the phases of S and G2/M in T24, T24/DOX, and T24/CIS cells (**Figure 2B**). Hence, we further explored the molecular mechanism underlying NTX-induced cell cycle

arrest in drug-resistant cell lines. The G0/G1-related proteins were measured by western blot, which revealed that NTX downregulated the expressions of c-Myc, Cyclin D1, CDK4, and CDK6 in T24/DOX and T24/CIS cells (**Figure 2C**). These results above suggested that NTX induced G0/G1 phase arrest of DOX-resistant and CIS-resistant bladder cancer cells dose-dependently.

### **NTX promotes apoptosis of DOX-resistant and CIS-resistant bladder cancer cells**

T24, T24/DOX, and T24/CIS cells were treated with NTX (0, 10, 20, and 40  $\mu$ M) for 48 h, followed by flow cytometric analysis (**Figure 3A**). As presented in **Figure 3B**, the apoptotic rates of T24 cells in NTX groups were (14.65 $\pm$ 1.47)%, (38.26 $\pm$ 7.21)%, and (58.35 $\pm$ 0.43)% of the total cells, compared with only (5.96 $\pm$ 0.58)% in control group (**Figure 3B**). As NTX concentration increased, the apoptotic rates of T24/DOX cells were (4.42 $\pm$ 0.92)%, (16.52 $\pm$ 0.48)%, (30.84 $\pm$ 0.17)%, and (53.37 $\pm$ 2.67)%, while the rates of T24/CIS cells were (6.05 $\pm$ 0.14)%, (14.49 $\pm$ 1.89)%, (53.19 $\pm$ 3.68)%, and (62.36 $\pm$ 2.51)%, respectively (**Figure 3B**). Consistent with the apoptosis trend detected by flow cytometry, Hoechst staining results indicated a higher proportion of apoptotic T24, T24/DOX, and T24/CIS cells in NTX-treated groups, exhibiting such typical morphological changes as chromatin condensation and nuclear fragmentations (**Figure 3C**).

Western blot analysis revealed that the levels of Bcl-xL, Mcl-1, and Survivin decreased following NTX treatment (**Figure 3D**). Our results indicated that NTX promoted the apoptosis of both DOX-resistant and CIS-resistant T24 cells.

### **NTX suppresses the STAT3 signaling and P-gp in T24/DOX and T24/CIS cells**

Western blot was applied to analyze whether NTX treatment regulated the expressions of proteins associated with STAT3 signaling and P-gp. **Figure 4A** illustrates that NTX significantly decreased the levels of STAT3, p-STAT3 (Y705), p-STAT3 (S727), and P-gp in a dose-dependent manner.

To further verify whether NTX induced apoptosis and G0/G1 arrest through the STAT3 signaling, T24/DOX and T24/CIS cells were incubated with NTX (10  $\mu$ M) or Stattic (4  $\mu$ M) for 24 h. Western blot analysis demonstrated that NTX (10  $\mu$ M, 24h or 48 h) or Stattic (4  $\mu$ M, 24h) alone did not significantly inhibit STAT3 expression, but higher concentrations of NTX (20 and 40  $\mu$ M) decreased the levels of STAT3 (**Figure 4A, B**). The combination of NTX and Stattic synergistically downregulated the expressions of p-STAT3 (Y705), P-gp, Cyclin D1, and Mcl-1 (**Figure 4B**). These findings suggested that NTX could inhibit P-gp, promote apoptosis and G0/G1 arrest in DOX-resistant and CIS-resistant T24 cell lines via the STAT3 pathway.

#### **NTX exhibits the anti-tumor effect in T24/DOX and T24/CIS tumor-bearing mice**

To determine the in vivo anti-tumor effect of NTX, we established the T24/DOX and T24/CIS tumor xenograft models, followed by oral administration of NTX (40 mg/kg) or PBS (vehicle group). The representative changes of tumors were shown in **Figure 5A, 6A**, showing a significantly lower tumor size in the treatment group than that in the control group. The average tumor weights were (0.272 $\pm$ 0.031) g for vehicle group and (0.095 $\pm$ 0.022) g for NTX group in T24/DOX model (**Figure 5B**), while those were (0.420 $\pm$ 0.121) g for vehicle group and (0.192 $\pm$ 0.072) g for NTX group in

T24/CIS model (**Figure 6B**). Similar for T24/DOX and T24/CIS models, the tumors grew slowly in NTX group when compared with the vehicle group (**Figure 5C, 6C**). No significant differences were found in the mean body weights of T24/DOX or T24/CIS tumor-bearing mice between NTX group and the corresponding control group (**Figure 5D, 6D**), indicating a low toxicity of NTX in vivo.

The morphological changes of H&E staining were shown in **Figure 5E, 6E**. The tumor cells in vehicle group were intact with deeply stained, large and abnormal nuclei, while those in NTX group presented with disappeared nuclei and tumor necrosis. Western blot analysis of T24/DOX and T24/CIS tumor tissues revealed that the expressions of p-STAT3 (Y705), p-STAT3 (S727), P-gp, and Mcl-1 were reduced by NTX treatment as compared to vehicle group, but there was no significant difference in STAT3 expression (**Figure 5F, 6F**).

## **Discussion**

The high rates of recurrence and progression require repeated cycles of chemotherapy for a long-term duration, and subsequently trigger frequent MDR in UBC, leading to poor prognosis and heavy economic burden [3, 7]. In this study, NTX was firstly discovered as a STAT3 signaling inhibitor to trigger G0/G1 cell cycle arrest, apoptosis, and reverse P-gp overexpression in drug-resistant UBC. T24/DOX and T24/CIS cells have been well-established for decades to apply for basic research on UBC drug resistance to DOX or CIS [29-31]. Following the confirmation of drug-resistant characteristics, we identified the overexpressions of STAT3 and P-gp in T24/DOX

and T24/CIS cells. Moreover, we demonstrated by XTT assay that T24/DOX and T24/CIS cells were resistant to DOX and CIS, respectively, while both of them were sensitive to NTX in a time- and dose-dependent manner.

The cell cycle progresses sequentially through G0/G1, S, G2, and M phases. Its dysregulation is one of the most frequent alterations during tumorigenesis and disease progression. Blockade of cell cycle progression is considered as an efficient strategy to eliminate cancer cells [32]. Recent studies have reported NTX arrests glioma and myeloma cells at G0/G1 stage [26, 33]. Flow cytometric analysis also indicated NTX treatment led to the G0/G1 accumulation of DOX- and CIS-resistant T24 cells, which could prevent their transmission to the resulting daughter cells. Promoting cell cycle progression is a major carcinogenic mechanism of the proto-oncogene c-Myc, which potentially binds to Cyclin D1 promoter and upregulates its expression [34]. As an allosteric regulator, Cyclin D1 forms a complex with cyclin-dependent kinase 4/6 (CDK4/6), and the active Cyclin D1-CDK4/CDK6 complex drives cell cycle transition from G1 to S phase [35]. We next demonstrated that NTX treatment downregulated c-Myc, Cyclin D1, CDK4, and CDK6, providing a molecular-level explanation for NTX-induced G0/G1 arrest in T24/DOX and T24/CIS cells.

As a type of programmed cell death, apoptosis is mainly characterized by such morphological changes as cell shrinkage, chromatin condensation, nuclear fragmentation [36]. Consistently, we observed these typical morphological changes in T24, T24/DOX, and T24/CIS cells following NTX treatment, which were further



confirmed by flow cytometric analysis. The B-cell lymphoma-2 (Bcl-2) family proteins are known as crucial regulators of mitochondria-mediated apoptosis, among which anti-apoptotic members such as myeloid cell leukemia 1 (Mcl-1), B-cell lymphoma-extra large (Bcl-xL) are well-validated anticancer targets [37]. As a member of the inhibitor of apoptosis (IAP) family, Survivin is overexpressed in multiple cancers, and its upregulation in cancer is associated with chemoresistance and radioresistance [38]. Western blot analysis revealed that NTX treatment downregulated the expressions of anti-apoptotic proteins Bcl-xL, Mcl-1, and Survivin.

Increasing evidence suggests that STAT3 plays a critical role in chemoresistance, proliferation, and apoptosis of multiple tumor cells [14]. Previous studies have also reported that STAT3 overexpression occurs in drug-resistant UBC cell lines and associates with poor prognosis of UBC patients [15, 16]. Therefore, inhibition of STAT3 signaling is a promising therapeutic strategy to decrease chemoresistance and induce apoptosis of drug-resistant UBC. Consistently, the expressions of STAT3 and P-gp were upregulated in T24/DOX and T24/CIS cells compared with T24 parental cells. After membrane surface receptors are stimulated by cytokines or growth factors, STAT3 can be activated to signal through both canonical and non-canonical pathways [39]. For the canonical pathway, the subsequent phosphorylation of STAT3 at Y705 residue will homodimerize or heterodimerize through their SH2 domains (**Figure 7A**). Then, STAT3 dimers translocate to the nucleus where they bind to promoter elements of target genes including the MDR1 gene, the cell cycle regulatory genes such as c-Myc, Cyclin D1, and the anti-apoptotic genes such as Survivin, Mcl-1, Bcl-xL, and

further modulate their transcription [40]. For the non-canonical pathway, the phosphorylation of STAT3 at S727 residue is required for maximal STAT3 activation [17]. The subsequent translocation of p-STAT3 (S727) to the mitochondria promotes tumor cell proliferation by reducing the production of reactive oxygen species (ROS), a mediator of cell apoptosis [41]. In this study, NTX was identified as a potent STAT3 inhibitor to downregulate the expressions of STAT3, p-STAT3 (Y705), and p-STAT3 (S727) in T24/DOX and T24/CIS cells. As shown in **Figure 7B**, we proposed the molecular mechanism for NTX-induced P-gp reversal, G0/G1 arrest, and apoptosis in T24/DOX and T24/CIS cells. NTX treatment downregulated the expressions of STAT3 and p-STAT3 (Y705), which subsequently decreased the translocation of STAT3 dimers into the nucleus. Then, the downstream target including MDR1 gene, the cell cycle regulatory genes such as c-Myc, Cyclin D1, and the anti-apoptotic genes such as Survivin, Mcl-1, Bcl-xL were downregulated, which could reverse MDR, trigger G0/G1 arrest, and induce apoptosis, respectively. Moreover, the downregulated p-STAT3 (S727) could promote ROS generation, which further mediated the apoptosis of T24/DOX and T24/CIS cells. According to the recent reports, there is still a huge controversy on whether p-STAT3 (S727) regulates p-STAT3 (Y705) negatively or positively [42-44], which needs further experimental confirmation. NTX and Stattic, a selective inhibitor of STAT3 activation and dimerization, synergistically decreased p-STAT3 (Y705), P-gp, and the anti-apoptotic member Mcl-1, which further verified NTX-mediated STAT3 inhibition in drug-resistant UBC.

Consistent with in vitro experiments, NTX treatment (40 mg/kg/day) for two

weeks exhibited a significant anti-tumor effect in T24/DOX and T24/CIS tumor-bearing mice. The dosage was selected based on the recommended dose for urinary tract infections [45], the guide for dose conversion between animals and human [46], and animal experiments in previous studies [23, 24]. The mean body weights of T24/DOX or T24/CIS tumor-bearing mice exhibited no significant difference between NTX group and the corresponding control group, which also indicated its favorable safety profile. Interestingly, by H&E staining, we also observed the disappeared nuclei and tumor necrosis in NTX group.

To our knowledge, this is the first report to discover NTX as a STAT3 inhibitor for drug-resistant UBC therapy. However, it should be noted that single agent therapy for UBC potentially leads to chemotherapy failure with limited therapeutic efficacy and drug resistance [47]. It remains to be investigated whether NTX or its analogues combined with DOX or CIS can enhance the anti-tumor effect, promote the extrusion of drugs into extracellular space by drug efflux pumps, and even delay the development of drug resistance in UBC without significantly increasing toxicity. Our previous work found that NTX induces tumor growth inhibition and decreases the levels of myeloid-derived suppressor cells (MDSCs) in a murine xenograft model of UBC [23]. Interestingly, Takeyama et al. recently reported the elevated expansion and infiltration of MDSCs in tumor microenvironment of CIS-resistant UBC [48]. Further studies are needed to identify whether MDSCs could be a novel target of NTX for the treatment of drug-resistant UBC.

## **Conclusions**

Here we reported for the first time that NTX as a STAT3 inhibitor exhibits the significant anti-tumor efficacy for drug-resistant UBC treatment in vitro and in vivo. Our observations demonstrated that NTX induces P-gp reversal, G0/G1 cell cycle arrest, and apoptosis in drug-resistant UBC via suppression of the STAT3 signaling pathway. Therefore, these findings could have significant clinical implications in developing NTX as a STAT3 inhibitor against drug-resistant UBC.

## **Abbreviations**

UBC: urothelial bladder cancer; MIBC: muscle-invasive bladder cancer; NMIBC: non-muscle-invasive bladder cancer; NTX: Nitroxoline; DOX/ADM/ADR: doxorubicin; CIS/DDP/CDDP: cisplatin; P-gp: P-glycoprotein; MDR: multidrug resistance; ABCB1: ATP-binding cassette B1; MDR1 gene: multidrug resistance 1 gene; STAT3: Signal transducer and activators of transcription 3; ChIP: chromatin immunoprecipitation; MetAP2: methionine aminopeptidase-2; EMT: epithelial-mesenchymal transition; PD-L1: programmed cell death ligand-1; PD-1: programmed cell death protein 1; H&E staining: hematoxylin and eosin staining; SD: standard deviation; IC50: half maximal inhibitory concentration; ANOVA: one-way analysis of variance; 95%CI: 95% confidence interval; CDK4/6: cyclin-dependent kinase 4/6; Mcl-1: myeloid cell leukemia 1; Bcl-xL: B-cell lymphoma-extra large; ROS: reactive oxygen species; MDSCs: myeloid-derived suppressor cells.

## **Competing interests**

The authors declare that they have no competing interests.

## **Funding**

This research was funded by the Ministry of Education, Culture, Sports, Science and Technology of Japan (grant No. 17K11138, 21K09371), and the China Scholarship Council.

## **Authors' contributions**

PH and YN conceived and supervised the study. WL and JS contributed to the study design and conducted most of the experiments. TS, NX, and KW interpreted data and

performed the statistical analysis. WL prepared the manuscript, while CL, MA, AX, and MW revised the manuscript. All authors read and approved the final manuscript.

### **Acknowledgments**

We thank Hideo Ueki and Shunai Li at Okayama University for their technical guidance.

## Reference

1. Oliveira MC, Caires HR, Oliveira MJ, Fraga A, Vasconcelos MH, Ribeiro R. Urinary Biomarkers in Bladder Cancer: Where Do We Stand and Potential Role of Extracellular Vesicles. *Cancers (Basel)*. 2020; 12.
2. Siegel RL, Miller KD, Fuchs HE, Jemal A. Cancer Statistics, 2021. *CA Cancer J Clin*. 2021; 71: 7-33.
3. Patel VG, Oh WK, Galsky MD. Treatment of muscle-invasive and advanced bladder cancer in 2020. *CA Cancer J Clin*. 2020; 70: 404-23.
4. Chaudhuri AA, Pellini B, Pejovic N, Chauhan PS, Harris PK, Szymanski JJ, et al. Emerging Roles of Urine-Based Tumor DNA Analysis in Bladder Cancer Management. *JCO Precis Oncol*. 2020; 4.
5. Leow JJ, Bedke J, Chamie K, Collins JW, Daneshmand S, Grivas P, et al. SIU-ICUD consultation on bladder cancer: treatment of muscle-invasive bladder cancer. *World J Urol*. 2019; 37: 61-83.
6. Gomez De Liano A, Duran I. The continuing role of chemotherapy in the management of advanced urothelial cancer. *Ther Adv Urol*. 2018; 10: 455-80.
7. Mollaei M, Hassan ZM, Khorshidi F, Langroudi L. Chemotherapeutic drugs: Cell death- and resistance-related signaling pathways. Are they really as smart as the tumor cells? *Transl Oncol*. 2021; 14: 101056.
8. Suzman DL, Agrawal S, Ning YM, Maher VE, Fernandes LL, Karuri S, et al. FDA Approval Summary: Atezolizumab or Pembrolizumab for the Treatment of Patients with Advanced Urothelial Carcinoma Ineligible for Cisplatin-Containing Chemotherapy. *Oncologist*. 2019; 24: 563-9.
9. Wang F, Li D, Zheng Z, Kin Wah To K, Chen Z, Zhong M, et al. Reversal of ABCB1-related multidrug resistance by ERK5-IN-1. *J Exp Clin Cancer Res*. 2020; 39: 50.
10. Nanayakkara AK, Follit CA, Chen G, Williams NS, Vogel PD, Wise JG. Targeted inhibitors of P-glycoprotein increase chemotherapeutic-induced mortality of multidrug resistant tumor cells. *Sci Rep*. 2018; 8: 967.
11. Choi YH, Yu AM. ABC transporters in multidrug resistance and pharmacokinetics, and strategies for drug development. *Curr Pharm Des*. 2014; 20: 793-807.
12. Bukowski K, Kciuk M, Kontek R. Mechanisms of Multidrug Resistance in Cancer Chemotherapy. *Int J Mol Sci*. 2020; 21.
13. He C, Sun Z, Hoffman RM, Yang Z, Jiang Y, Wang L, et al. P-Glycoprotein Overexpression Is Associated With Cisplatin Resistance in Human Osteosarcoma. *Anticancer Res*. 2019; 39: 1711-8.
14. Loh CY, Arya A, Naema AF, Wong WF, Sethi G, Looi CY. Signal Transducer and Activator of Transcription (STATs) Proteins in Cancer and Inflammation: Functions and Therapeutic Implication. *Front Oncol*. 2019; 9: 48.
15. Chen Z, Chen X, Xie R, Huang M, Dong W, Han J, et al. DANCR Promotes Metastasis and Proliferation in Bladder Cancer Cells by Enhancing IL-11-STAT3 Signaling and CCND1 Expression. *Mol Ther*. 2019; 27: 326-41.
16. Gatta LB, Melocchi L, Bugatti M, Missale F, Lonardi S, Zanetti B, et al. Hyper-Activation of STAT3 Sustains Progression of Non-Papillary Basal-Type Bladder Cancer via FOSL1 Regulome. *Cancers (Basel)*. 2019; 11.
17. Yang J, Kunimoto H, Katayama B, Zhao H, Shiromizu T, Wang L, et al. Phospho-Ser727 triggers a multistep inactivation of STAT3 by rapid dissociation of pY705-SH2 through C-terminal tail modulation. *Int Immunol*. 2020; 32: 73-88.
18. Ji L, Liu X, Zhang S, Tang S, Yang S, Li S, et al. The Novel Triazolonephthalimide Derivative LSS-11

Synergizes the Anti-Proliferative Effect of Paclitaxel via STAT3-Dependent MDR1 and MRP1 Downregulation in Chemoresistant Lung Cancer Cells. *Molecules*. 2017; 22.

19. Zhang X, Xiao W, Wang L, Tian Z, Zhang J. Deactivation of signal transducer and activator of transcription 3 reverses chemotherapeutics resistance of leukemia cells via down-regulating P-gp. *PLoS One*. 2011; 6: e20965.

20. Thilakasiri PS, Dmello RS, Nero TL, Parker MW, Ernst M, Chand AL. Repurposing of drugs as STAT3 inhibitors for cancer therapy. *Semin Cancer Biol*. 2021; 68: 31-46.

21. Talevi A, Bellera CL. Challenges and opportunities with drug repurposing: finding strategies to find alternative uses of therapeutics. *Expert Opin Drug Discov*. 2020; 15: 397-401.

22. Shim JS, Matsui Y, Bhat S, Nacev BA, Xu J, Bhang HE, et al. Effect of nitroxoline on angiogenesis and growth of human bladder cancer. *J Natl Cancer Inst*. 2010; 102: 1855-73.

23. Xu N, Lin W, Sun J, Sadahira T, Xu A, Watanabe M, et al. Nitroxoline inhibits bladder cancer progression by reversing EMT process and enhancing anti-tumor immunity. *J Cancer*. 2020; 11: 6633-41.

24. Zhang QI, Wang S, Yang D, Pan K, Li L, Yuan S. Preclinical pharmacodynamic evaluation of antibiotic nitroxoline for anticancer drug repurposing. *Oncol Lett*. 2016; 11: 3265-72.

25. Veschi S, De Lellis L, Florio R, Lanuti P, Massucci A, Tinari N, et al. Effects of repurposed drug candidates nitroxoline and nelfinavir as single agents or in combination with erlotinib in pancreatic cancer cells. *J Exp Clin Cancer Res*. 2018; 37: 236.

26. Lazovic J, Guo L, Nakashima J, Mirsadraei L, Yong W, Kim HJ, et al. Nitroxoline induces apoptosis and slows glioma growth in vivo. *Neuro Oncol*. 2015; 17: 53-62.

27. Mari A, D'Andrea D, Abufaraj M, Foerster B, Kimura S, Shariat SF. Genetic determinants for chemo- and radiotherapy resistance in bladder cancer. *Transl Androl Urol*. 2017; 6: 1081-9.

28. Vallo S, Michaelis M, Rothweiler F, Bartsch G, Gust KM, Limbart DM, et al. Drug-Resistant Urothelial Cancer Cell Lines Display Diverse Sensitivity Profiles to Potential Second-Line Therapeutics. *Transl Oncol*. 2015; 8: 210-6.

29. Byun SS, Kim SW, Choi H, Lee C, Lee E. Augmentation of cisplatin sensitivity in cisplatin-resistant human bladder cancer cells by modulating glutathione concentrations and glutathione-related enzyme activities. *BJU Int*. 2005; 95: 1086-90.

30. Kim WT, Kim J, Yan C, Jeong P, Choi SY, Lee OJ, et al. S100A9 and EGFR gene signatures predict disease progression in muscle invasive bladder cancer patients after chemotherapy. *Ann Oncol*. 2014; 25: 974-9.

31. Tanaka M, Koul D, Davies MA, Liebert M, Steck PA, Grossman HB. MMAC1/PTEN inhibits cell growth and induces chemosensitivity to doxorubicin in human bladder cancer cells. *Oncogene*. 2000; 19: 5406-12.

32. Lin W, Xie J, Xu N, Huang L, Xu A, Li H, et al. Glaucocalyxin A induces G2/M cell cycle arrest and apoptosis through the PI3K/Akt pathway in human bladder cancer cells. *Int J Biol Sci*. 2018; 14: 418-26.

33. Li G, Zheng YH, Xu L, Feng J, Tang HL, Luo C, et al. BRD4 inhibitor nitroxoline enhances the sensitivity of multiple myeloma cells to bortezomib in vitro and in vivo by promoting mitochondrial pathway-mediated cell apoptosis. *Ther Adv Hematol*. 2020; 11: 2040620720932686.

34. Garcia-Gutierrez L, Delgado MD, Leon J. MYC Oncogene Contributions to Release of Cell Cycle Brakes. *Genes (Basel)*. 2019; 10.

35. Qie S, Diehl JA. Cyclin D1, cancer progression, and opportunities in cancer treatment. *J Mol Med*



(Berl). 2016; 94: 1313-26.

36. Tang D, Kang R, Berghe TV, Vandenamee P, Kroemer G. The molecular machinery of regulated cell death. *Cell Res.* 2019; 29: 347-64.
37. Hata AN, Engelman JA, Faber AC. The BCL2 Family: Key Mediators of the Apoptotic Response to Targeted Anticancer Therapeutics. *Cancer Discov.* 2015; 5: 475-87.
38. Rathore R, McCallum JE, Varghese E, Florea AM, Busselberg D. Overcoming chemotherapy drug resistance by targeting inhibitors of apoptosis proteins (IAPs). *Apoptosis.* 2017; 22: 898-919.
39. Zhang ZH, Li MY, Wang Z, Zuo HX, Wang JY, Xing Y, et al. Convallatoxin promotes apoptosis and inhibits proliferation and angiogenesis through crosstalk between JAK2/STAT3 (T705) and mTOR/STAT3 (S727) signaling pathways in colorectal cancer. *Phytomedicine.* 2020; 68: 153172.
40. Laudisi F, Cherubini F, Monteleone G, Stolfi C. STAT3 Interactors as Potential Therapeutic Targets for Cancer Treatment. *Int J Mol Sci.* 2018; 19.
41. Meier JA, Hyun M, Cantwell M, Raza A, Mertens C, Raje V, et al. Stress-induced dynamic regulation of mitochondrial STAT3 and its association with cyclophilin D reduce mitochondrial ROS production. *Sci Signal.* 2017; 10.
42. Huang G, Yan H, Ye S, Tong C, Ying QL. STAT3 phosphorylation at tyrosine 705 and serine 727 differentially regulates mouse ESC fates. *Stem Cells.* 2014; 32: 1149-60.
43. Mandal T, Bhowmik A, Chatterjee A, Chatterjee U, Chatterjee S, Ghosh MK. Reduced phosphorylation of Stat3 at Ser-727 mediated by casein kinase 2 - protein phosphatase 2A enhances Stat3 Tyr-705 induced tumorigenic potential of glioma cells. *Cell Signal.* 2014; 26: 1725-34.
44. Wakahara R, Kunimoto H, Tanino K, Kojima H, Inoue A, Shintaku H, et al. Phospho-Ser727 of STAT3 regulates STAT3 activity by enhancing dephosphorylation of phospho-Tyr705 largely through TC45. *Genes Cells.* 2012; 17: 132-45.
45. Wagenlehner FM, Munch F, Pilatz A, Barmann B, Weidner W, Wagenlehner CM, et al. Urinary concentrations and antibacterial activities of nitroxoline at 250 milligrams versus trimethoprim at 200 milligrams against uropathogens in healthy volunteers. *Antimicrob Agents Chemother.* 2014; 58: 713-21.
46. Nair AB, Jacob S. A simple practice guide for dose conversion between animals and human. *J Basic Clin Pharm.* 2016; 7: 27-31.
47. Alfarouk KO, Stock CM, Taylor S, Walsh M, Muddathir AK, Verduzco D, et al. Resistance to cancer chemotherapy: failure in drug response from ADME to P-gp. *Cancer Cell Int.* 2015; 15: 71.
48. Takeyama Y, Kato M, Tamada S, Azuma Y, Shimizu Y, Iguchi T, et al. Myeloid-derived suppressor cells are essential partners for immune checkpoint inhibitors in the treatment of cisplatin-resistant bladder cancer. *Cancer Lett.* 2020; 479: 89-99.

**Table 1 IC50 values\* of DOX, CIS, or NTX determined in T24, T24/DOX and T24/CIS cells.**

	T24		T24/DOX		T24/Cis	
	IC50 (μM)	95%CI	IC50 (μM)	95%CI	IC50 (μM)	95%CI
DOX (24 h)	0.71	0.56-0.89	10.93	6.88-17.55	-	-
CIS (24 h)	16.27	13.29-19.11	-	-	58.04	51.11-67.55
NTX (24 h)	15.22	12.77-18.19	14.91	12.99-17.02	19.72	18.11-21.53
NTX (48h)	7.85	7.15-8.61	10.69	9.31-12.27	11.20	10.17-12.30
NTX (72h)	4.48	4.17-4.82	7.32	6.55-8.16	9.15	8.09-10.27

\*IC50 values represent the concentrations of DOX, CIS, or NTX producing 50% cell growth inhibition. Abbreviations: IC50, half maximal inhibitory concentration; 95%CI: 95% confidence interval; DOX: doxorubicin; CIS: cisplatin; NTX: nitroxoline.

### Figure legends

**Figure 1 T24/DOX and T24/CIS cells were resistant to DOX and CIS, respectively, but sensitive to NTX.**

(A) T24 and T24/DOX cells were treated with different concentrations of DOX (0, 0.1, 1, 10, 20, or 100 μM) for 24 h, followed by the evaluation of cell viability using XTT assay. (B) T24 and T24/CIS cells were treated with different concentrations of CIS (0, 10, 20, 40, or 80 μM) for 24 h, followed by the evaluation of cell viability using XTT assay. Data are expressed as the mean ± SD (n=6). \**P* < 0.05 vs T24 parental cells. (C) The expression levels of STAT3 and P-gp in T24, T24/DOX, and T24/CIS cells were analyzed by western blot analysis. β-actin was used as a loading control. (D) T24, (E) T24/DOX, and (F) T24/CIS cells were exposed to different concentrations of NTX (0, 2.5, 5, 10, 20, and 40 μM) for 24, 48, and 72 h. The cell viability was determined by XTT assay. Data are shown as the mean ± SD (n=6). \**P* < 0.05 vs the control group.

**Figure 2 NTX triggers G0/G1 phase cell cycle arrest in T24, T24/DOX, and T24/CIS cells.**

(A) T24, T24/DOX, and T24/CIS cells were treated with the indicated concentrations of NTX (0, 10, 20, and 40  $\mu$ M) for 24 h. The harvested cells were incubated with PI/RNase, followed by flow cytometric analysis of cell cycle distribution. (B) The proportions of cells in each phase (G0/G1, S, and G2/M) are presented in the histograms. Data are expressed as the mean  $\pm$  SD from three independent experiments. \* $P < 0.05$  vs the control group. (C) T24/DOX and T24/CIS cells were treated with NTX (0, 10, 20, and 40  $\mu$ M) for 48 h. Proteins were extracted and western blot was used to analyze the expressions of c-Myc, Cyclin D1, CDK4, and CDK6.  $\beta$ -actin was used as a loading control.

**Figure 3 NTX induces apoptosis of T24, T24/DOX, and T24/CIS cells.**

(A) T24, T24/DOX, and T24/CIS cells were treated with the indicated concentrations of NTX (0, 10, 20, and 40  $\mu$ M) for 48 h. The cells were stained with Annexin V-FITC/PI and flow cytometry was used to analyze the apoptotic rates. (B) T24, T24/DOX, and T24/CIS cells were treated with the indicated concentrations of NTX (0, 10, 20, and 40  $\mu$ M) for 48 h. The percentages of apoptotic cells are shown in the histograms. Data are expressed as the mean  $\pm$  SD from three independent experiments. \* $P < 0.05$ , \*\*\* $P < 0.001$  vs the control group. (C) The indicated concentrations of NTX (0 and 40  $\mu$ M) were used to treat T24, T24/DOX, and T24/CIS cells for 48 h. Hoechst 33342 was then used to stain the cell nuclei (blue), followed by fluorescence microscopy. Scale bar = 100  $\mu$ m. (D) T24/DOX and T24/CIS cells were treated with NTX (0, 10, 20, and 40  $\mu$ M) for 48 h, followed by western blot to assess the expressions of Bcl-xL, Mcl-1, and Survivin.  $\beta$ -actin was used as a loading control.

**Figure 4 NTX suppresses the STAT3 signaling pathway in T24/DOX and T24/CIS cells.**

(A) Western blot was used to assess the expressions of STAT3, p-STAT3 (Y705), p-STAT3 (S727), and P-gp in T24, T24/DOX, and T24/CIS cells after they were treated with NTX (0, 10, 20, and 40  $\mu$ M) for 48 h. (B) T24/DOX and T24/CIS cells were exposed to 10  $\mu$ M NTX in the presence or absence of 4  $\mu$ M Stattic for 24 h. Western blot was then performed to detect the expressions of STAT3, p-STAT3 (Y705), P-gp, Cyclin D1, and Mcl-1.

**Figure 5 NTX exhibits the anti-tumor effect on T24/DOX in vivo.**

(A) T24/DOX tumors were excised from mice and photographed after two-week treatment. (B) The average tumor weight of NTX treatment group significantly decreased compared with that of vehicle group. (C) The growth curves of T24/DOX tumors at the indicated days following NTX treatment. (D) No significant difference was found in the body weight of T24/DOX tumor-bearing mice between treatment group and vehicle group. Data are expressed as the mean  $\pm$  SD. \*\*\* $P < 0.001$ , ns:  $P > 0.05$ , vs the vehicle group. (E) H&E staining was performed to observe the morphological alterations in T24/DOX tumors after NTX treatment. Scale bar = 50  $\mu$ m. (F) Proteins were extracted from T24/DOX tumors and western blot was used to detect the expressions of STAT3, p-STAT3 (Y705), p-STAT3 (S727), P-gp, and Mcl-1.

**Figure 6 NTX exhibits the anti-tumor effect on T24/CIS in vivo.**

(A) T24/CIS tumors were excised from mice and photographed after two-week treatment. (B) The average tumor weight of NTX treatment group significantly

decreased compared with that of vehicle group. (C) The growth curves of T24/CIS tumors at the indicated days following NTX treatment. (D) No significant difference was found in the body weight of T24/CIS tumor-bearing mice between treatment group and vehicle group. Data are expressed as the mean  $\pm$  SD.  $**P < 0.01$ ,  $***P < 0.001$ , ns:  $P > 0.05$ , vs the vehicle group. (E) H&E staining was performed to observe the morphological alterations in T24/CIS tumors after NTX treatment. Scale bar = 50  $\mu\text{m}$ . (F) Proteins were extracted from T24/CIS tumors and western blot was used to detect the expressions of STAT3, p-STAT3 (Y705), p-STAT3 (S727), P-gp, and Mcl-1.

**Figure 7 Proposed mechanism for NTX-induced P-gp reversal, G0/G1 arrest and apoptosis in drug-resistant T24 cells.**

(A) The molecular structure of STAT3. (B) STAT3 can be activated to signal through both canonical and non-canonical pathways. For the canonical pathway, NTX inhibits STAT3 phosphorylation at Y705 residue and then decreases the translocation of STAT3 dimers to the nucleus in T24/DOX and T24/CIS cells. The subsequent downregulation of target genes including MDR1 gene, the cell cycle regulatory genes such as c-Myc, Cyclin D1, and the anti-apoptotic genes such as Survivin, Mcl-1, Bcl-xL, will reverse P-gp, trigger G0/G1 arrest, and induce apoptosis, respectively. For the non-canonical pathway, NTX-downregulated STAT3 phosphorylation at S727 residue reduces the translocation of p-STAT3 (S727) to the mitochondria and finally induces cell apoptosis by the increased generation of reactive oxygen species (ROS).

**Figure 1**

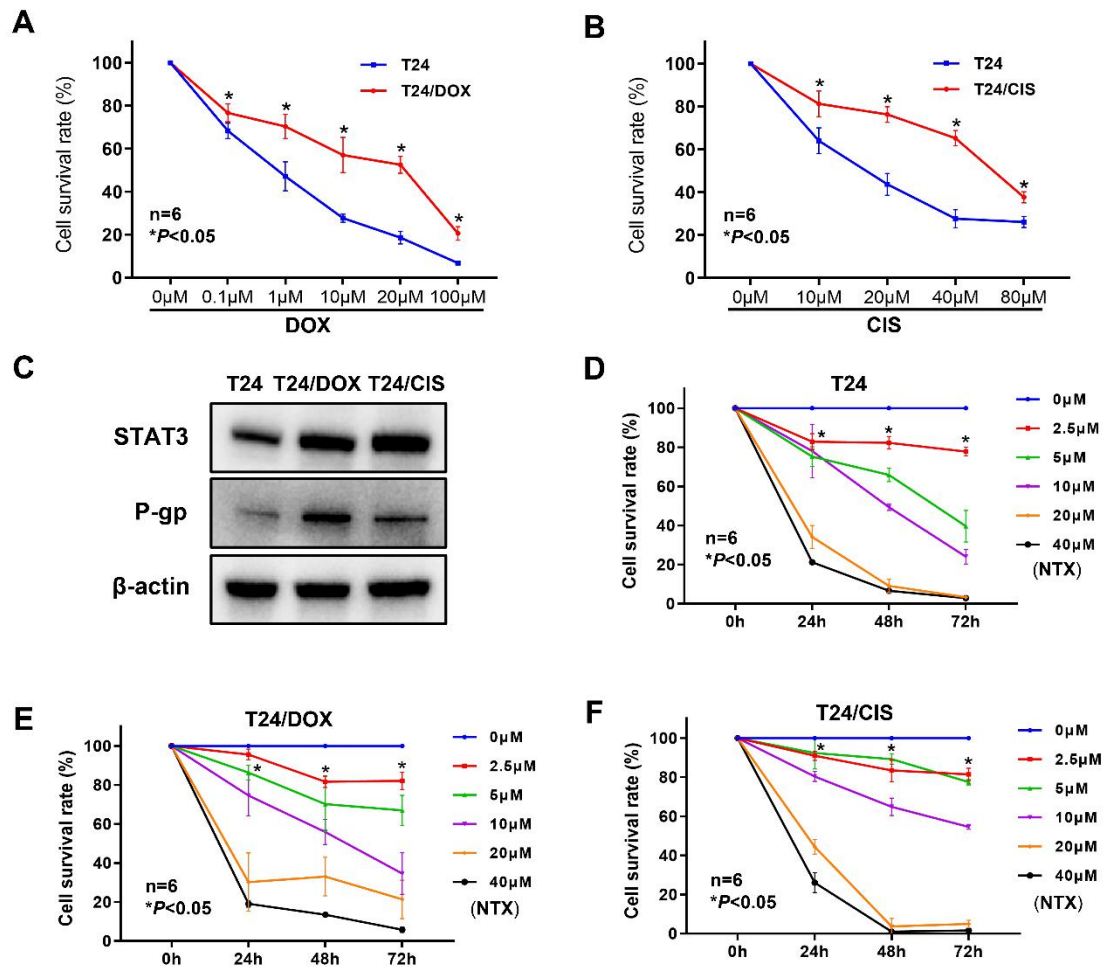
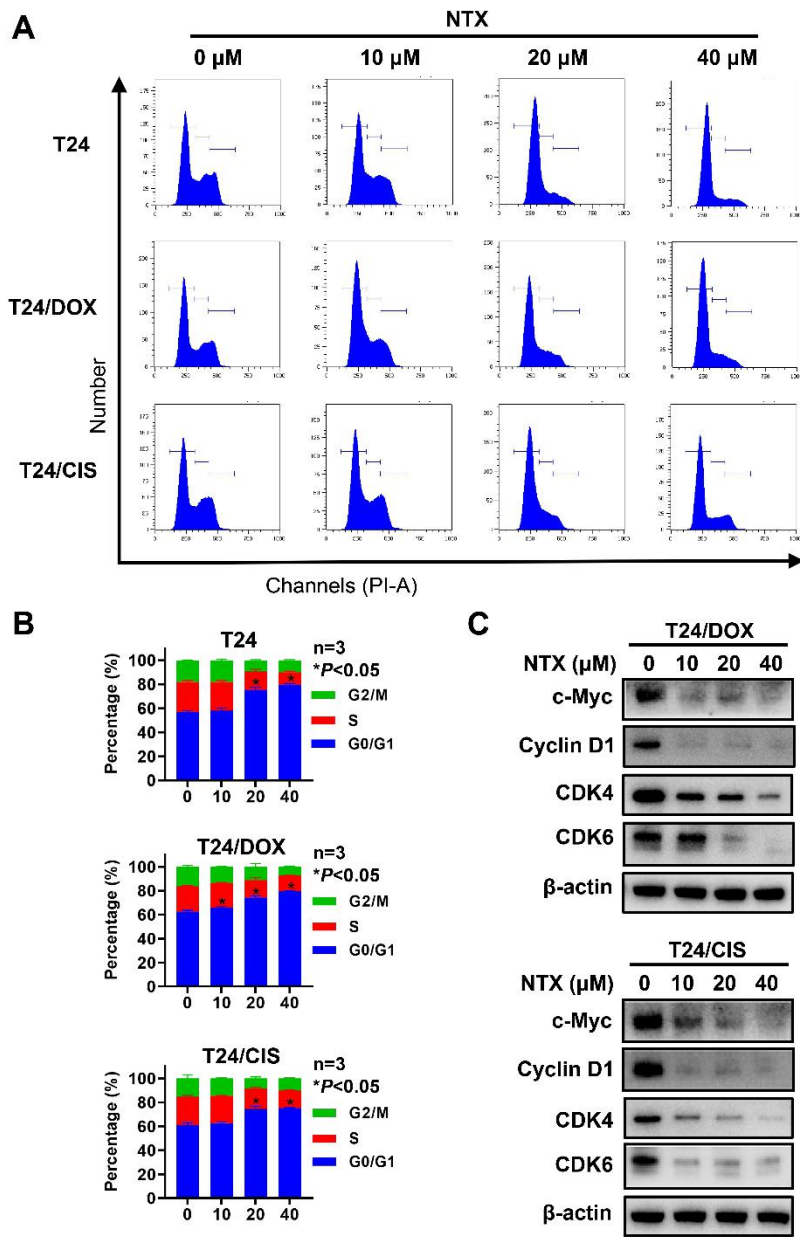
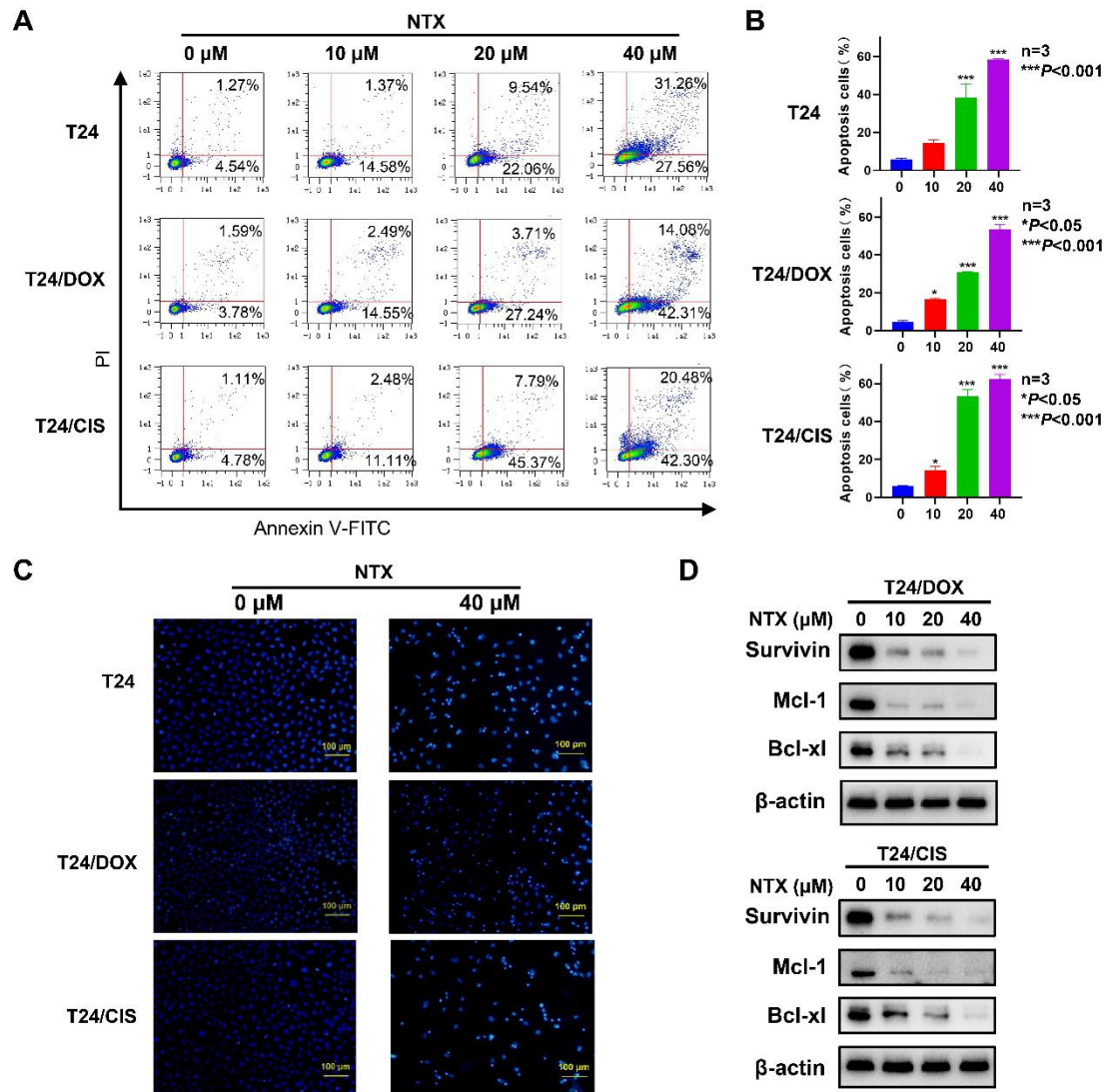


Figure 2



**Figure 3**





**Figure 4**

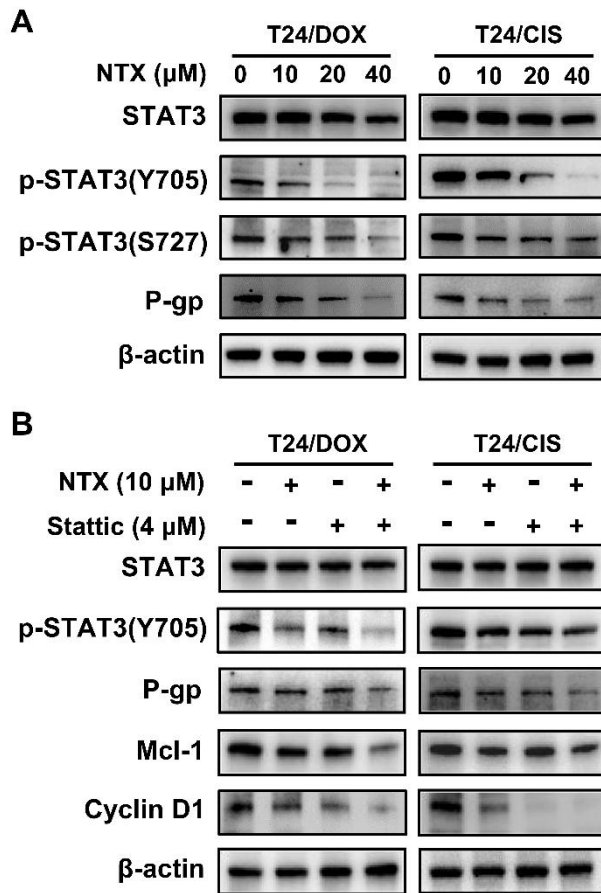


**Figure 5**

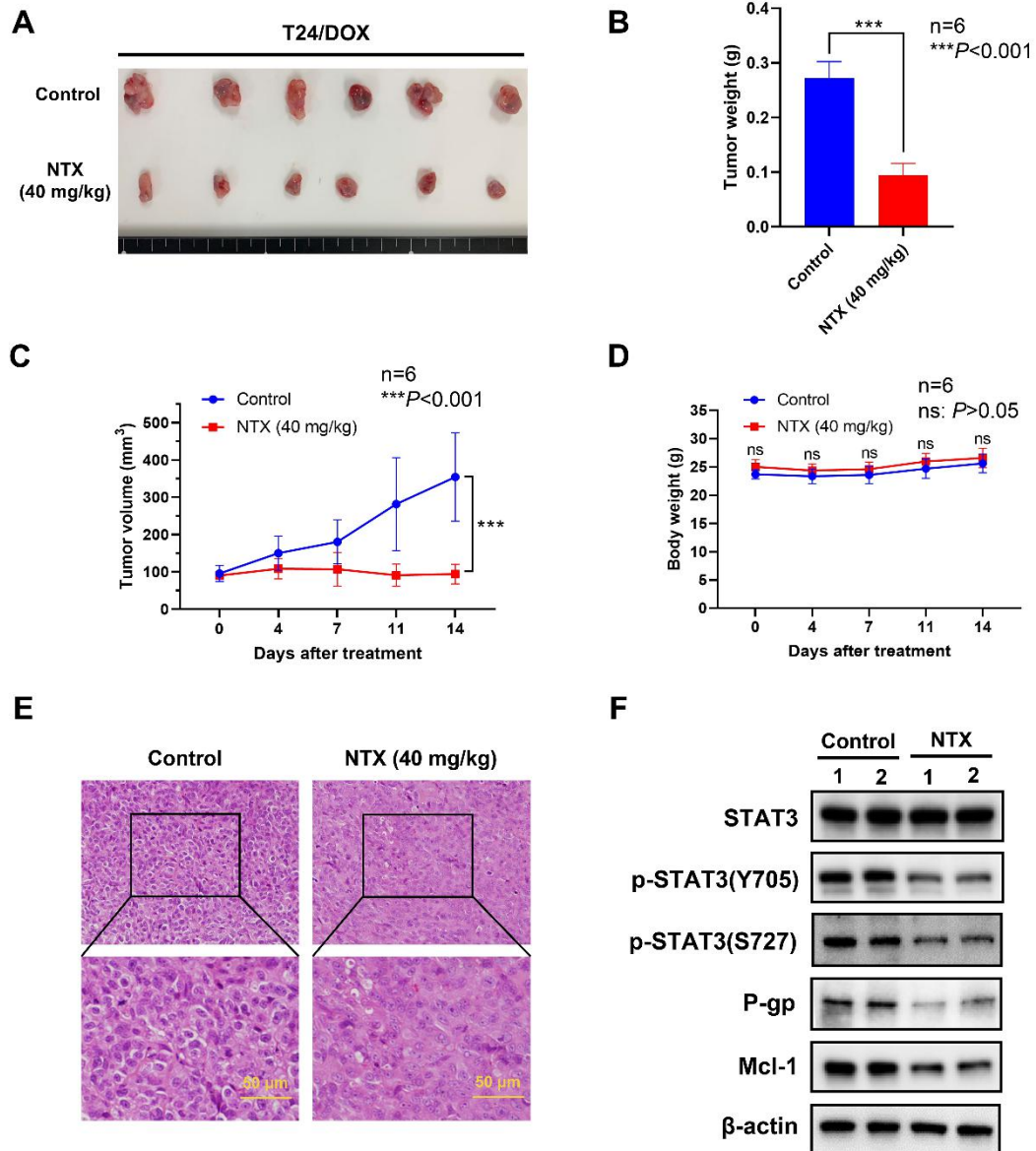


**Figure 6**

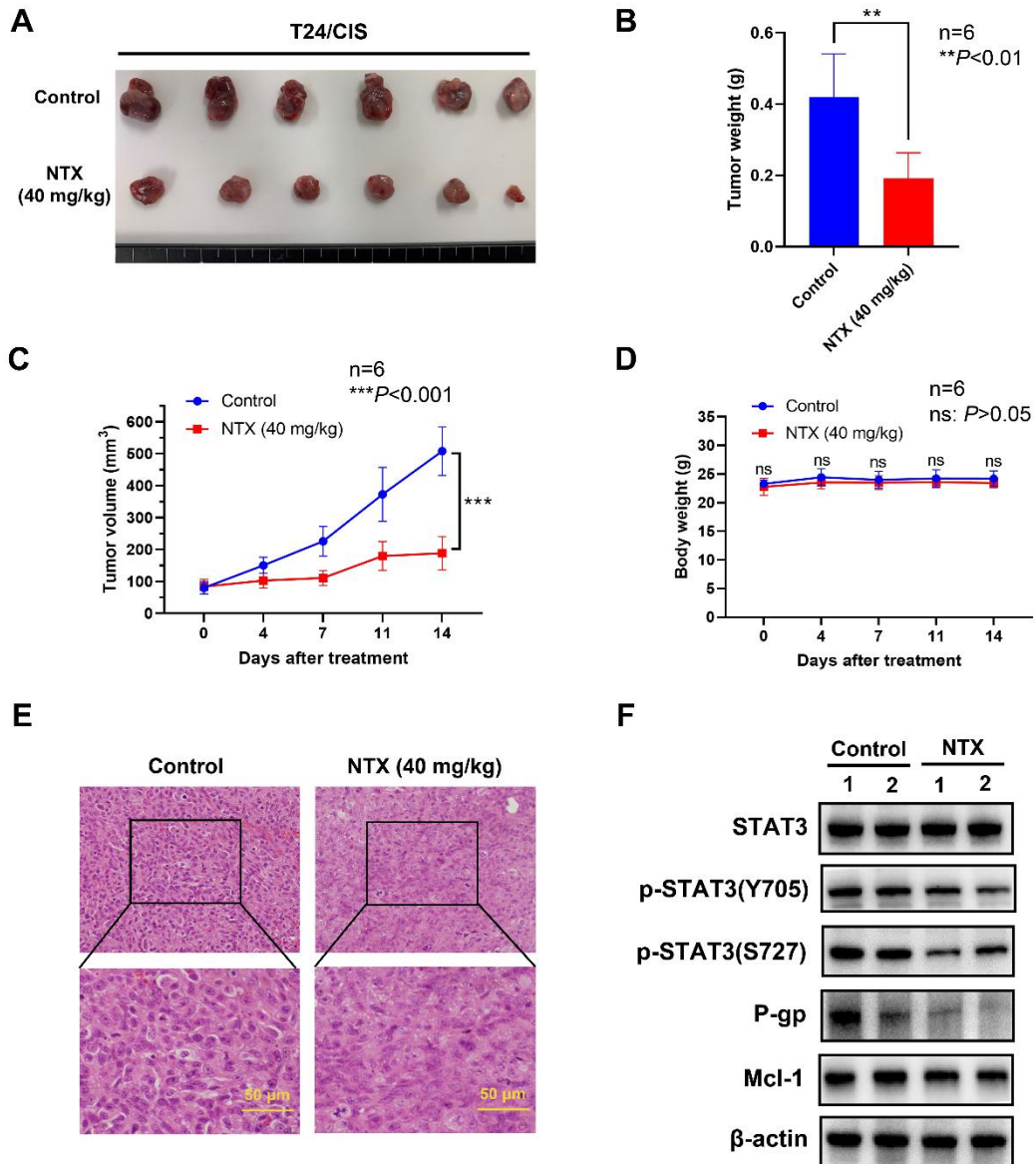


Figure 7

